International Journal of Pharmaceutics 404 (2011) 289–300

Contents lists available at ScienceDirect

International Journal of Pharmaceutics

journal homepage: www.elsevier.com/locate/ijpharm

Pharmaceutical Nanotechnology

Spray-freeze-drying production of thermally sensitive polymeric nanoparticle aggregates for inhaled drug delivery: Effect of freeze-drying adjuvants

Wean Sin Cheow, Mabel Li Ling Ng, Katherine Kho, Kunn Hadinoto*

School of Chemical and Biomedical Engineering, Nanyang Technological University, Singapore 637459, Singapore

ARTICLE INFO

Article history:
Received 10 September 2010
Received in revised form 28 October 2010
Accepted 11 November 2010
Available online 18 November 2010

Keywords:
Spray freeze drying
Poly(caprolactone)
Dry powder inhaler
Coalescence
Nanoparticles

ABSTRACT

Inhalable dry-powder aggregates of drug-loaded thermally sensitive poly(caprolactone) (PCL) nanoparticles are produced using spray-freeze-drying (SFD) as the low melting point of PCL prohibits the use of high-temperature spray-drying. The effects of freeze-drying adjuvant formulation on the particle morphology, aerodynamic diameter, aqueous re-dispersibility, flowability, and production yield are examined using mannitol and poly(vinyl alcohol) (PVA) as the adjuvants. The primary role of the adjuvant is to prevent irreversible nanoparticle coalescences during freeze-drying, thereby the nanoparticle aggregates can readily re-disperse into primary nanoparticles in an aqueous environment hence retaining their therapeutic functions. The nanoparticle aggregates produced using either adjuvant exhibit large, porous, and spherical morphologies suitable for dry-powder-inhaler delivery. The nanoparticle aggregates exhibit good flowability and effective aerosolization off the inhaler. The adjuvant selection governs the resultant nanoparticle–adjuvant structures, where PCL nanoparticles are physically dispersed in porous mannitol matrix, whereas PVA are coated onto the nanoparticle surface. Importantly, nanoparticle aggregates produced by SFD exhibit significantly higher aqueous re-dispersibility than those produced by spray-drying, which signifies the suitability of SFD as the method to produce solid-dosage-form of thermally sensitive nanoparticles. Overall, using PVA as adjuvant leads to more stable morphology, superior aqueous re-dispersibility, and higher production yield compared to the mannitol formulation.

1. Introduction

Dry powder inhaler (DPI) represents an effective pulmonary delivery platform for direct dosing of therapeutic agents to the lungs because of its portability, long shelf-life, and high delivery efficiency. These characteristics of DPI are in contrast to the relative inconvenience (e.g. lengthy treatment time, non-portability) and low delivery efficiency associated with the more conventional nebulization delivery platform. The use of nanoparticles as therapeutic carriers in DPI delivery has recently gained significant interest as nano-scale formulations enable the therapeutic agents to evade the lung phagocytic clearance and enhances the dissolution rate of poorly water-soluble drugs (Rogueda and Traini, 2007).

Direct inhalation of dry-powder nanoparticles, however, is not plausible because nanoparticles have a strong tendency to agglomerate resulting in difficult physical handling. Furthermore, nanoparticles, with the exception of particles <50 nm in size, are predominantly exhaled from the lung without depositing due to their low aerodynamic diameters (d_A) (Rogueda and Traini, 2007). In this regard, inhaled particles should possess d_A defined in Eq. (1) between 1 and 5 μm to effectively deposit in the lungs.

$$d_A = d_G\sqrt{\frac{\rho_e}{\rho_S}} \quad (1)$$

where d_G is the particle geometric diameter, $\rho_S = 1\ \mathrm{g/cm^3}$, and ρ_e is the particle effective density defined as the mass of particles divided by their total volume including the open and closed pores.

To facilitate their delivery by inhalation, nanoparticles are typically transformed by spray drying into low-density micro-scale nanoparticle aggregates (i.e. nano-aggregates) with large d_G (>5 μm) and low ρ_e ($\ll 1\ \mathrm{g/cm^3}$) using various pharmaceutical excipients as drying adjuvants (Grenha et al., 2005; Hadinoto and Cheow, 2009; Sham et al., 2004; Sung et al., 2009). The large d_G of the nano-aggregates alleviates the problem of particle agglomerations resulting in effective aerosolization off the inhaler, without the need for coarse carrier particle inclusion, and improved physical handling. Their low ρ_e, which is owed to either hollow or porous morphologies, ensures their d_A to fall within the range suitable for effective lung depositions despite the large d_G. Another advantage of this carrier-free DPI formulation is in eliminating the concern of poor liberations of drug particles from carrier particles observed in the conventional DPI formulation.

* Corresponding author. Tel.: +65 6514 8381; fax: +65 6794 7553.
E-mail address: kunnong@ntu.edu.sg (K. Hadinoto).

0378-5173/$ – see front matter © 2010 Elsevier B.V. All rights reserved.
doi:10.1016/j.ijpharm.2010.11.021

Nomenclature

ρ_e	effective density
ρ_S	unit density
ρ_{tap}	tap density
ρ_{bulk}	bulk density
CI	Carr's index
d_A	aerodynamic diameter
d_G	geometric diameter
ED	emitted dose
FPF	fine particle fraction
IP	induction port
N/M	nanoparticle to mannitol ratio
N/P	nanoparticle to PVA ratio
NGI	next generation impactor
PS	pre-separator
S_f	size of particles present in suspension after SFD
S_i	initial size of nanoparticles before SFD
SPET	standardized powder entrainment tube
Yield	production yield

The spray dryer is typically operated at inlet temperatures ≥100 °C to achieve a fast convective drying rate needed to obtain the low ρ_e. Exposure to high temperatures in the spray dryer, where the outlet spray-dryer temperatures vary in the range of 60–70 °C, however, is prohibitive when low melting-point or thermally sensitive biodegradable polymers, such as poly(caprolactone) (PCL) and poly(propylene succinate), are employed as therapeutic carriers. The high temperature can jeopardize the structural integrity of the nanoparticles, even in the presence of drying adjuvants, leading to nanoparticle degradations or coalescences that diminish their therapeutic functions.

The detrimental effects of the high temperature in a spray-drying process have been demonstrated in our earlier study (Kho et al., 2010) in which PCL nanoparticles were spray dried using mannitol, lactose, and leucine as drying adjuvants. PCL, a low melting point polymer (62 °C), has been widely studied as potential therapeutic carriers attributed to its high matrix permeability towards a wide range of therapeutic agents and its high physical stability owed to its highly crystalline structures (Sinha et al., 2004). Even though the nano-aggregates produced exhibited d_A in the range ideal for inhaled delivery, less than half of the nanoparticles were recovered from the nano-aggregates upon re-dispersion. The poor aqueous re-dispersibility of the spray-dried PCL nano-aggregates was caused by irreversible nanoparticle coalescences, where PCL nanoparticles softened and fused together upon exposure to temperature near or above their melting point.

Owing to its non-elevated temperature operation, spray freeze drying (SFD) represents a viable alternative to spray drying to produce dry-powder nano-aggregates. In terms of its applications, SFD has primarily been employed to produce dry-powder proteins as the sub-zero temperature, unlike the high temperature, does not adversely affect protein structures and functions (Costantino et al., 2000; Maa et al., 1999). SFD has also been used to produce solid dosage forms of poorly water-soluble drugs (Hu et al., 2002; Niwa et al., 2009) and to transform aqueous suspensions of drug-loaded liposomes into their dry-powder forms using lactose, sucrose, and mannitol as freeze-drying adjuvants (Bi et al., 2008; Sweeney et al., 2005). To the best of our knowledge, the use of SFD to transform aqueous suspensions of biodegradable polymeric nanoparticles into their inhalable dry-powder form has never been examined.

The two-step SFD process (i.e. atomization into a cryogen followed by lyophilization) to produce nano-aggregates is illustrated in Fig. 1. The first step involves channeling of the nanoparticle suspension through a nozzle to be atomized into tiny droplets. As the nanoparticle suspension is atomized into droplets, the cold temperature provided by the cryogen (i.e. liquid nitrogen) is sufficient to freeze water molecules present within the air-borne droplets. The droplets are completely frozen when they are immersed in the liquid nitrogen. The rapid freezing allows the water molecules to be frozen into ice crystals that are interspersed among the dissolved or suspended materials consisting of nanoparticles and freeze-drying adjuvants. Excess liquid nitrogen is subsequently removed from the slurry containing the frozen droplets by evaporation or decanting. The evaporation of the liquid nitrogen is carried out by holding the slurry at a temperature between the boiling point of the liquid nitrogen and the melting point of ice (i.e. between −196 °C and 0 °C) to ensure the droplets remain frozen while the liquid nitrogen is being evaporated.

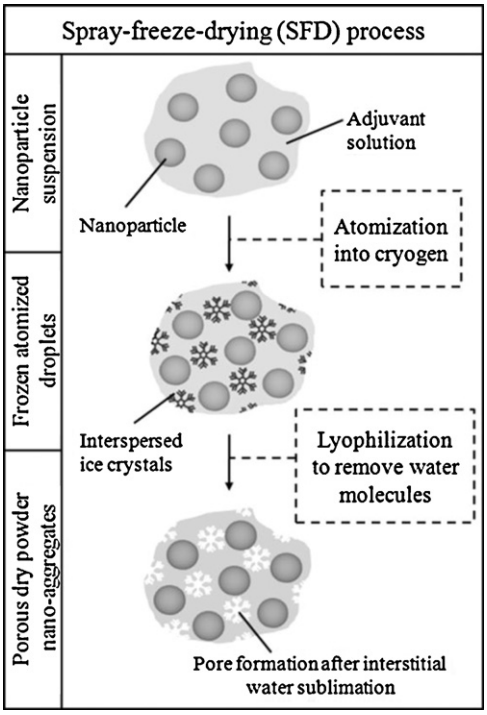

Fig. 1. Physical mechanisms of the spray-freeze-drying (SFD) process.

To obtain dry powders, the ice crystals are removed from the frozen droplets via sublimation in the lyophilization stage. The sublimation is carried out below the triple point of water (6 mbar, 0.01 °C) to prevent the melting of ice crystals into liquid water that can destroy the solid structure of the nano-aggregates. As the ice crystals in the frozen droplets are sublimed interstitially, the frozen droplets retain their size and do not shrink upon sublimation. Therefore, for identical atomizing conditions, SFD produces particles having larger d_G compared to spray drying in which the atomized droplets shrink due to convective evaporation of the aqueous medium. Furthermore, due to the interstitial sublimation, particles produced by SFD exhibit highly porous structures attributed to the presence of voids previously occupied by the sublimed ice crystals. As a result, nano-aggregates having large d_G and low ρ_e are straightforwardly produced by SFD.

In SFD of nanoparticle suspension, freeze-drying adjuvants need to be included in the formulation (i) to function as cryoprotective agents protecting the nanoparticles from the sub-zero temperature, and (ii) to facilitate re-dispersions of the nano-aggregates back into primary nanoparticles, so that the nanoparticles can perform their intended therapeutic functions. In inhaled drug deliv-

ery, aqueous re-dispersibility is an important characteristic of the micro-scale nano-aggregates as they must readily disassociate into primary nanoparticles upon exposure to the lung interstitial fluid in order to avoid lung phagocytosis that is least effective for particles smaller than 1–2 μm (Chono et al., 2006). In this regard, the adjuvant inclusion prevents the nanoparticles from forming irreversible coalescences upon freezing caused by mechanical stresses exerted by the ice crystal formation. The presence of adjuvants leads to the formation of "adjuvant bridges" that interconnect the nanoparticles hence preventing direct inter-nanoparticle contacts upon freezing. As a result, the nano-aggregate aqueous re-dispersibility is governed by the dissolution rate of the "adjuvant bridges" instead of the intrinsic attractive forces (e.g. van der Waals).

The objective of the present work is to examine the effects of freeze-drying adjuvant formulation on the morphology, aerodynamic diameter, aqueous re-dispersibility, flowability, and production yield of PCL nano-aggregates produced by SFD. Four generally recognized-as-safe (GRAS) excipients (i.e. mannitol, lactose, poly(vinyl alcohol) or PVA, and leucine), which have been widely studied for inhaled dosage form formulations, are used. The PCL nanoparticles are loaded with antibiotics (i.e. levofloxacin) to represent a model of aerosol antibiotic formulation intended for lung biofilm infection therapy, where nano-scale therapeutic carriers have been found to be superior to their micro-scale counterparts attributed to the nanoparticle ability to penetrate the airway sputum (Lai et al., 2009).

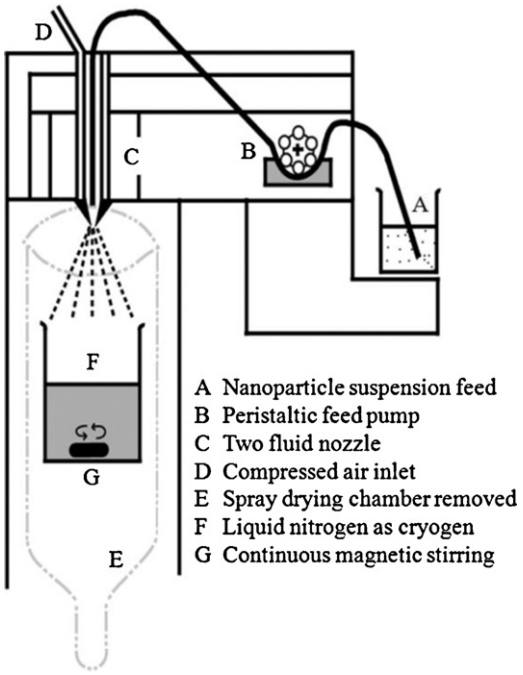

Fig. 2. A schematic representation of the SFD set-up.

2. Materials and methods

2.1. Materials

PCL (MW = 80,000), levofloxacin, and dichloromethane (DCM) used in the nanoparticle preparation and the adjuvants (i.e. L-leucine, PVA (MW = 23,000), α-lactose monohydrates, and D-mannitol) are purchased from Sigma–Aldrich (USA). Leucine is a hydrophobic compound, whose inclusion results in particles having corrugated surfaces, hence better particle entrainment off the inhaler (Minne et al., 2008). PVA, a biodegradable and non-cytotoxic surfactant, has been found to be a suitable lyoprotectant for PCL nanocapsules (Abdelwahed et al., 2006a). Mannitol and lactose have often been used as coarse carrier particles in DPI (Rowe et al., 2009).

2.2. Methods

2.2.1. Preparation of drug-loaded PCL nanoparticles

Briefly, 80 mg of drug and 800 mg of PCL are dissolved in 20 mL of DCM. A 2 mL aliquot of this solution is poured into a 6 mL aqueous solution of 1.0% (w/v) PVA, and the resulting immiscible two-phase liquid system is emulsified for 60 s using a Vibra-Cell probe sonicator (VC 5040, Sonics and Materials, USA). The nano-emulsion is next added to a 100 mL aqueous solution of 0.1% (w/v) PVA. The sonication process is repeated for the remaining 18 mL of PCL–drug solution, and the resultant nano-emulsion is similarly added to the 100 mL of 0.1% (w/v) PVA solution. The suspension is stirred overnight at room temperature to evaporate off the DCM. The resulting nanoparticle suspension is then centrifuged twice at 11,000 RPM to remove the non-encapsulated drug and excess PVA.

2.2.2. Physical characterizations of drug-loaded PCL nanoparticles

The initial size of the nanoparticles before SFD (S_i) is measured by photon correlation spectroscopy (PCS) using a Brookhaven 90Plus Nanoparticle Size Analyzer (Brookhaven Instruments Corporation, USA). The drug encapsulation efficiency (i.e. % encapsulation) is determined from the ratio of the amount of the encapsulated drug to the amount of drug initially added. The amount of the encapsulated drug is determined by subtracting the drug amount present in the supernatant after centrifugation from the amount of drug initially added. The drug concentration in the supernatant is measured using UV-VIS spectrophotometer (UV Mini-1240, Shimadzu, Japan) at absorbance wavelength of 254 nm. Experimental uncertainty in the % encapsulation is ≈7%.

2.2.3. Spray-freeze-drying of drug-loaded PCL nanoparticle suspension

The feed suspension is prepared by adding drug-loaded PCL nanoparticles into aqueous solutions of the adjuvants. SFD is performed in a modified BÜCHI B-290 mini spray-dryer (BÜCHI, Switzerland) as illustrated in Fig. 2, where the drying chamber of the spray dryer is removed and replaced with a polypropylene vessel containing 500 mL of liquid nitrogen under constant stirring. As preliminary experiments show that the use of ultrasonic atomizer (Vibracell VC 5040, Sonics and Materials, USA) led to the freezing of the feed solution in the nozzle, a two-fluid atomizer having 1.5 mm nozzle diameter is used instead. The feed is atomized into liquid nitrogen with the nozzle positioned 10 cm above the liquid nitrogen level. The following three parameters are kept constant i.e. 0.24 L/h feed rate, 240 L/h atomizing air flow rate, and 500 RPM liquid nitrogen stirring speed.

Following atomization, the slurry containing the frozen droplets and the remaining liquid nitrogen is transferred to a lyophilization container, and the excess liquid nitrogen is evaporated. The freezing is continued at −80 °C for 16 h after which lyophilization is carried out for 24 h in a Alpha 1-2 LD Plus freeze dryer (Martin Christ, Germany) at a temperature of −52 °C and a vacuum level of 0.05 mbar resulting in dry-powder production. The production yield is determined from the ratio of the nano-aggregate mass recovered after SFD to the initial mass added in the feed (i.e. PCL and adjuvant).

2.2.4. Physical characterizations of spray-freeze-dried PCL nano-aggregates

2.2.4.1. Particle morphology. The nano-aggregate morphology is characterized using a scanning electron microscope (SEM) model JSM-6700F (JEOL, USA) equipped with energy dispersive X-ray spectroscopy (EDX) to verify the presence of adjuvant in the spray-freeze-dried particles. As the nano-aggregates are specifically designed to re-disperse into primary nanoparticles in an aqueous medium, d_G of the nano-aggregates is determined by image analysis instead of laser diffraction-based sizing method, which employs high-intensity wet dispersion methods to break particle agglomerates prior to measurements. The wet dispersion method is unfavourable for sizing the nano-aggregates because it would lead to inaccurate d_G measurements due to premature nano-aggregates re-dispersions. In the image analysis, SEM images of the nano-aggregates are analysed using ImageJ software (NIH, USA), where sixplicates of 1000 particles are measured for each sample. The number-based size distribution from the image analysis is converted to the volume-based distribution yielding the reported d_G values. Experimental uncertainties in the d_G values are ±7%.

2.2.4.2. Particle density, aerodynamic diameter, and flowability. ρ_e of the nano-aggregates is determined from the tap density (ρ_{tap}) values obtained from two replicates of 1 mL particle volume each, where each sample is subjected to 2000 taps in a tap densitometer (Quantachromme, USA). The d_G and ρ_e values are subsequently used to calculate theoretical d_A using Eq. (1). Experimental uncertainties in the d_A values are ≈8% based on the experimental errors in the d_G and ρ_{tap} measurements. The particle flowability is characterized by Carr's compressibility index (CI) defined in Eq. (2) using the bulk (ρ_{bulk}) and ρ_{tap} values, where weighed amount of powders is loosely filled into a 5 mL measuring cylinder to determine ρ_{bulk}. CI ≤ 25 and CI ≥ 40 are indicative of free-flowing and poorly flowable particles, respectively (Podczeck, 1998).

$$CI = \left(1 - \frac{\rho_{bulk}}{\rho_{tap}}\right) \times 100\% \quad (2)$$

Experimental uncertainties in the calculated CI values are ≈7% based on the experimental errors in the ρ_{bulk} and ρ_{tap} measurements.

In addition, particle flowability upon aerosolization is examined in terms of the emitted dose (ED) and fine particle fraction (FPF) using Next Generation Pharmaceutical Impactor (NGI) (Copley Scientific, UK) equipped with an induction port and a pre-separator. ED is defined as the percentage mass of powders that are emitted off the inhaler, whereas FPF is defined as the percentage mass of powders recovered in the impactor that possess $d_A \leq 5$ μm. Standardized powder entrainment tube (SPET) detailed in Louey et al. (2006) is adopted in the aerosolization characterization study in place of an inhaler. In this regard, aerosolization characteristics of powders delivered by SPET have been shown to be comparable to those delivered by two commercial inhaler devices (i.e. Rotahaler and Inhalator) as manifested by their similar ED, FPF, and mass median aerodynamic diameter (MMAD) values (Louey et al., 2006).

The inhalation flow rate needed to achieve the standard 4 kPa pressure drop in SPET is 85 L/min measured using a critical flow controller (Copley Scientific, UK). The air flow duration is set to 2.8 s to simulate a typical inhalation volume of 4 L. The effective cut-off diameters at 85 L/min are 6.7, 3.7, 2.4, 1.4, and 0.3 for stages 1–5, respectively. The impactor plates are coated with silicone grease (Dow Corning®) to prevent particle re-entrainments. The amount of powders recovered in each stage is determined from the amount of adjuvants recovered by means of colorimetric assays (Finley, 1961; Sanchez, 1998) using UV-VIS spectrophotometer. ED and FPF measurements are performed in triplicates using 5 mg of powders each time. Experimental uncertainties in the ED and FPF values are ≈8% and 5%, respectively.

2.2.4.3. Aqueous re-dispersibility. Conventional characterization methods for aqueous re-dispersions, which involve homogenization or sonication, are not employed in the present work as high intensity dispersion forces do not represent the actual re-dispersion mechanism in the epithelial lining fluid of the lungs. Instead, spontaneous aqueous re-dispersion characterization method is employed. Briefly, 10 mg of the dry-powder nano-aggregates are added to 1 mL of deionized water and the suspension is let sit for 10 min. The size of the particles present in the suspension (S_f) is measured afterwards by PCS and the ratio of S_f/S_i is calculated to determine the extent of the re-dispersion, where ratio of $S_f/S_i \approx 1$ signifies complete aggregate re-dispersions into primary nanoparticles.

To determine the mass fraction of nano-aggregates that have re-dispersed during the 10 min-period (i.e. % re-dispersed), the suspension is centrifuged at 6000 RPM for 1 min after which 1.5 mL of the supernatant, which contains the dissolved adjuvants and the re-dispersed nanoparticles, is removed and replaced with 1.5 mL of deionized water without stirring. The resulting suspension is centrifuged for the second time. The dilution and centrifugation are repeated two more times to ensure the removal of all the re-dispersed nanoparticles and the dissolved adjuvants. After the fourth centrifugation, 1.5 mL of the supernatant is discarded and the remaining 0.5 mL sedimented pellets are lyophilized for 24 h. The lyophilized pellets, which contain the nano-aggregates that have not re-dispersed, are weighed. The three cycles of centrifugation and re-suspension ensure the dissolution of a majority of the water-soluble adjuvants. Therefore, the % re-dispersed is determined from the ratio of the lyophilized pellet weight to the initial PCL nanoparticle weight in the feed.

3. Results and discussion

3.1. Drug-loaded PCL nanoparticle characteristics

Drug-loaded PCL nanoparticles are produced with diameter (S_i) of 290 ± 40 nm and the % encapsulation is low at ≈8% due to the high aqueous solubility of the model drug (≈100 mg/mL), which causes a majority of the drug diffuse out into the aqueous phase during the emulsification and solvent evaporation steps. In this regard, % encapsulation of water-soluble drugs in hydrophobic polymeric nanoparticles can be enhanced by modifying the nanoparticle preparation method (e.g. using alternative solvents and surfactants, w/o/w double emulsification) (Cheow and Hadinoto, 2010; Misra et al., 2009; Sheikh et al., 2009). Improving the % encapsulation, however, is not pursued in the present work as the emphasis is on examining the effects of adjuvant formulation on the physical characteristics of spray-freeze-dried nano-aggregates.

3.2. Adjuvant screening

In the absence of adjuvants, PCL nanoparticle suspension at 5.0% (w/v) concentration can be transformed into dry-powder nano-aggregates using SFD. Fig. 3a shows the large and spherical morphologies of the spray-freeze-dried nano-aggregates ($d_G \gg 10$ μm). Importantly, the large d_G is still smaller than the secondary bronchial diameter that is in the half-millimeter range. A closer look at the particle surface in Fig. 3b reveals porous structures manifested in the low particle density ($\rho_{tap} \approx 0.05$ g/cm^3). The particle geometric size distribution shown in Fig. 3c indicates a rather wide distribution between 10 and 60 μm with mean $d_G \approx 18$ μm. Despite the large d_G, d_A of the nano-aggregates remains in the

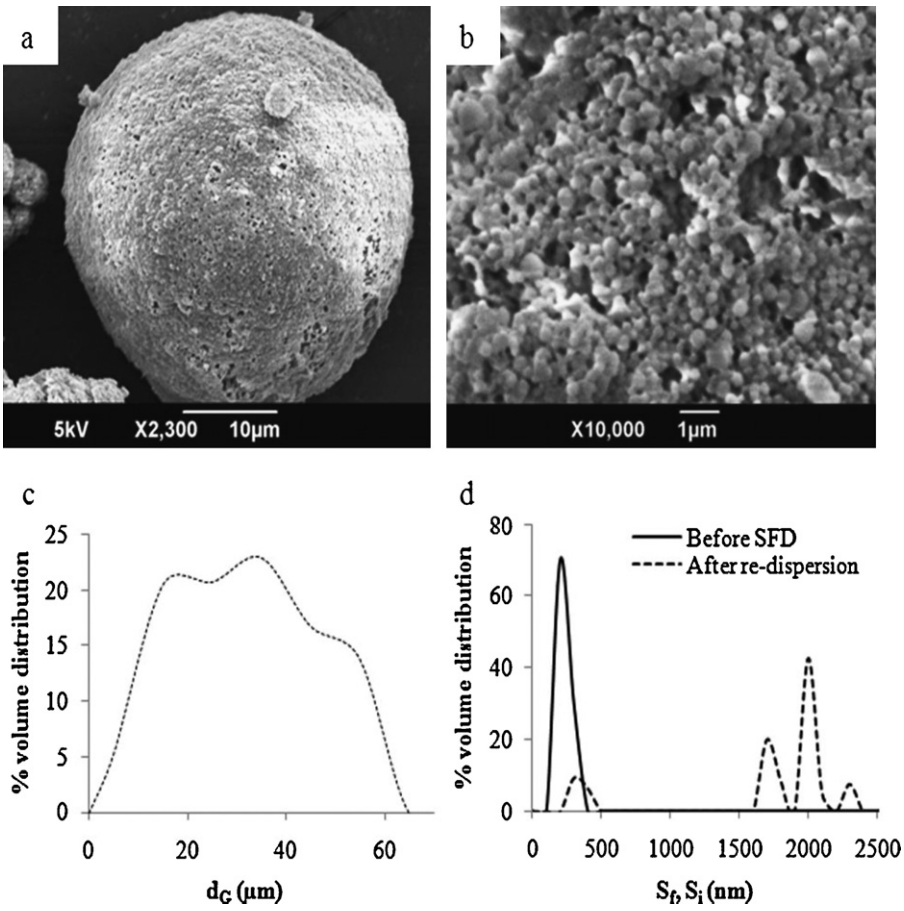

Fig. 3. (a) Large and spherical morphologies of PCL nano-aggregates, (b) PCL nanoparticles on the surface, (c) geometric particle size distribution, and (d) size distribution of PCL nanoparticles before SFD and after re-dispersion in an aqueous medium.

≈4–5 μm range owed to the low particle density hence they are suitable for lung depositions.

In terms of the aqueous re-dispersibility shown in Fig. 3d, however, approximately only 20% of the nano-aggregates are recovered as primary nanoparticles upon aqueous re-dispersion. A majority of the nano-aggregates are recovered as aggregate fragments, whose sizes are in the 1500–2500 nm range, indicating poor aqueous re-dispersibility manifested in the high ratio of S_f/S_i (≈5). The results of the adjuvant-free formulation indicate that adjuvants must be added to facilitate aqueous re-dispersions of the nano-aggregates. To assess the suitability of lactose, leucine, mannitol, and PVA as SFD adjuvants, their aqueous solutions are spray-freeze-dried in the absence of PCL nanoparticles. Fig. 4a–c shows the morphology of particles produced from SFD of 7.0% (w/v) aqueous solutions of lactose, mannitol, and PVA, respectively. SFD of leucine in Fig. 4d is conducted at a lower concentration of 1.5% (w/v) due to its lower aqueous solubility limit.

The results of the PCL-free formulation indicate that the high hygroscopicity of lactose leads to the production of highly cohesive particles (Fig. 4a) that leads to poor flowability. The use of lactose as the adjuvant is therefore ruled out. On the contrary, SFD of both mannitol and PVA solutions lead to the production of non-cohesive spherical particles shown in Fig. 4b and c, respectively, where PVA particles exhibit smooth surfaces and mannitol particles exhibit highly porous structures. Not unexpectedly, PVA particles exhibit a higher density (ρ_{tap} = 0.09 g/cm^3) than that of the mannitol particles (ρ_{tap} = 0.07 g/cm^3). In contrast, SFD of the leucine solution produces irregularly shaped and fragile fragments (Fig. 4d), where intact leucine particles are rarely observed. The results of the adjuvant screening therefore suggest that mannitol and PVA are the two most promising SFD adjuvant candidates. The effects of mannitol and PVA inclusions on the morphology, aqueous re-dispersibility, flowability, and production yield of the PCL nano-aggregates are investigated next.

3.3. Mannitol as adjuvants

The effects of adjuvant formulation are investigated by varying the nanoparticle to mannitol concentration ratio (i.e. N/M ratio) at two total solid concentrations (i.e. 5.0% and 2.5%, w/w) in the feed. The results of experimental runs at 5.0% (w/w) (i.e. Runs A1–A4) and at 2.5% (w/w) (i.e. Runs B1–B4) are presented in Table 1. The N/M ratios are varied by varying mannitol concentration in the feed between 20% and 70% (w/w). Using mannitol as adjuvant, SFD at feed concentrations lower than 2.5% (w/w) produces fragile particles that are not likely to withstand the aerosolization force. On the other hand, SFD at higher solid concentrations than 5.0% (w/w) produces large but non-porous particles, such that they do not satisfy the $d_A \approx 1$–5 μm requirement.

3.3.1. Morphology, density, aerodynamic diameter, flowability, and production yield

In the absence of mannitol, the results in Table 1 indicate that nano-aggregates produced at 5.0% (w/w) feed concentration (i.e. Run A1) exhibit higher ρ_{tap} and slightly larger d_G than Run B1 at 2.5% (w/w) feed concentration. This observation is not unexpected as similar trends have been observed in SFD of aqueous solutions (Her et al., 2010). In the presence of mannitol, a similar trend in d_G is observed in which nano-aggregates produced at a higher feed concentration exhibit larger d_G (i.e. 25–40 μm in Runs A2–A4 versus

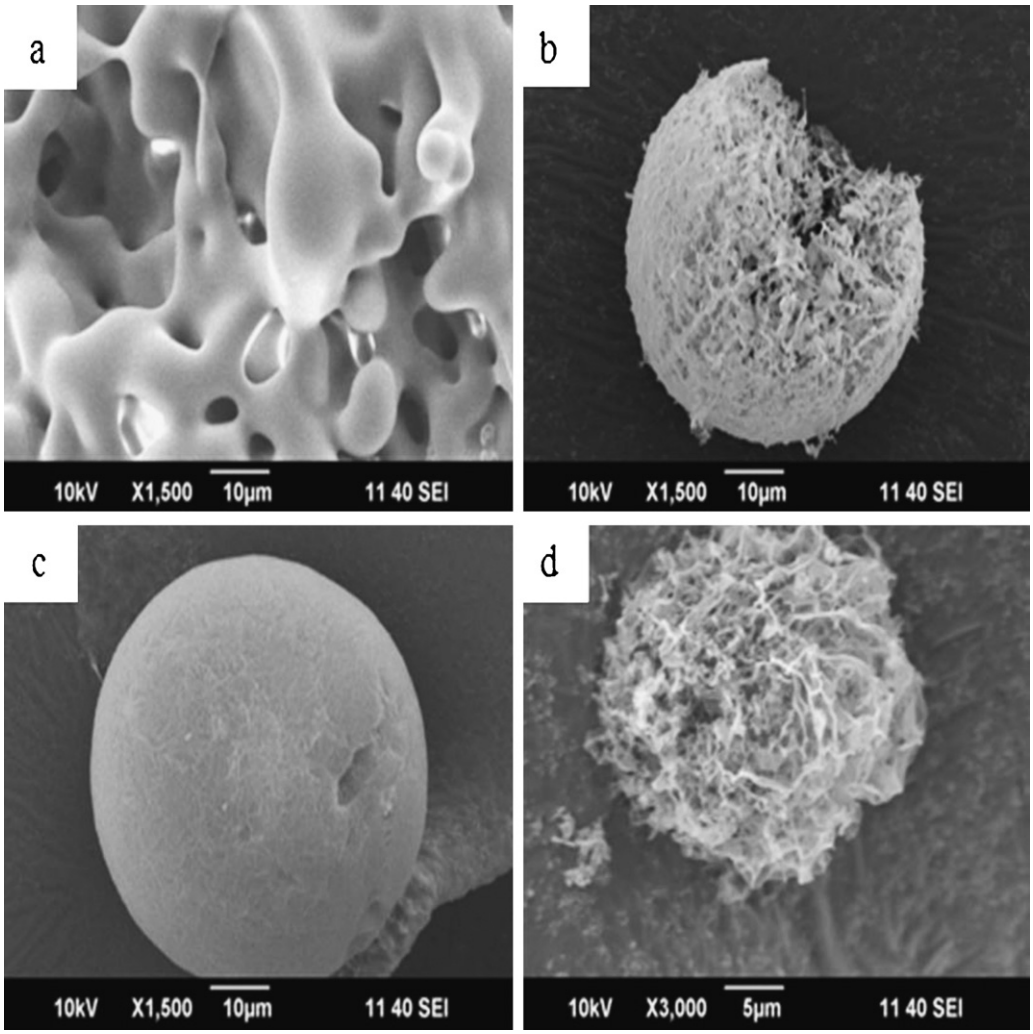

Fig. 4. Morphologies of spray-freeze-dried (a) lactose, (b) mannitol, (c) PVA, and (d) leucine.

20–25 μm in Runs B2–B4). Significantly, nano-aggregates produced from the mannitol-free formulations (i.e. Runs A1 and B1) exhibit higher ρ_{tap} and smaller d_G compared to those produced with mannitol at the same feed concentration. These results indicate that more porous and larger nano-aggregates are produced with the mannitol inclusion. In addition, the production yields are reduced from ≈60–70% in the mannitol-free formulations to ≈15–40% in the presence of mannitol depending on the mannitol concentration.

SEM image of the PCL–mannitol nano-aggregates in Fig. 5a reveals their large and highly porous morphologies. A close-up view of the particle surface in Fig. 5b indicates that PCL nanoparticles are physically dispersed in porous mannitol matrix, such that the nanoparticles are not in direct contacts with each other. High nano-aggregate aqueous re-dispersibility is therefore expected. In the presence of mannitol, the d_G values increase with increasing mannitol concentrations in the feed (i.e. lower N/M ratio) as larger porous mannitol particles are produced. The trends in ρ_{tap} and production yield as a function of the N/M ratio are less predictable. Importantly, despite the variations in the d_G and ρ_{tap} values, the d_A values in Runs A2–A4 and B2–B4 remain relatively constant as a function of the mannitol concentration as shown in Fig. 6a.

Owing to their larger d_G, nano-aggregates produced at 5.0% (w/w) feed concentration consistently exhibit larger d_A compared to those produced at 2.5% (w/w) feed concentration. Specifically, the former attains d_A of ≈4.0–5.0 μm and the latter attains slightly smaller d_A at ≈2.5–3.5 μm. Both of them therefore satisfy the d_A requirement for effective lung depositions. In terms of the flowability, CI values of the nano-aggregates produced in Runs A1–A4

Table 1
Summary of PCL–mannitol nano-aggregate experiments.

Run	Feed conc. (w/w)	% mannitol (w/w)	N/M ratio	ρ_{tap} (g/cm^3)	d_G (μm)	Yield (%)
A1	5.0%	0	–	0.052	18	58
A2		20	4:1	0.034	25	41
A3		40	3:2	0.014	35	15
A4		70	3:7	0.016	41	26
B1	2.5%	0	–	0.044	16	70
B2		20	4:1	0.017	20	16
B3		40	3:2	0.014	23	13
B4		70	3:7	0.019	25	40

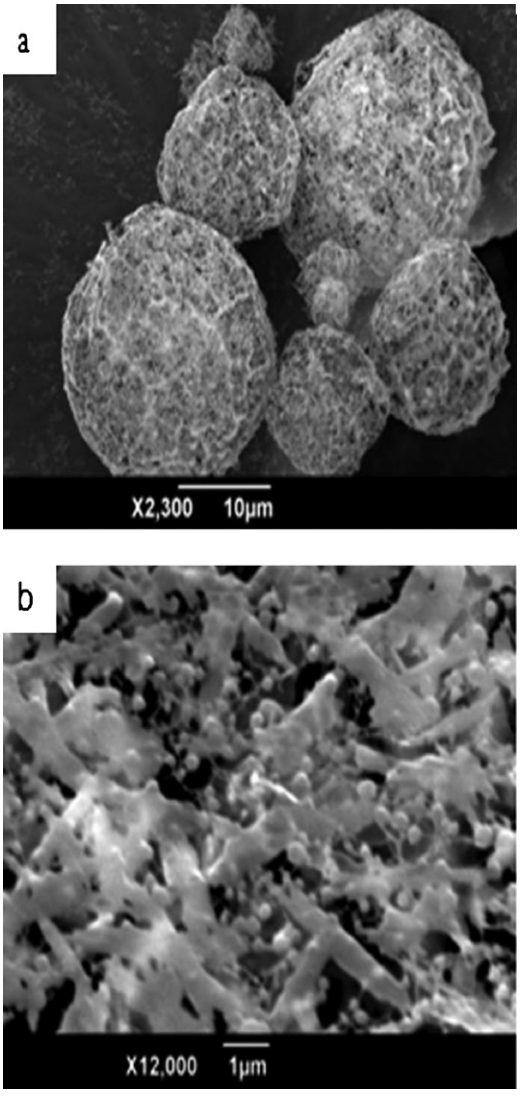

Fig. 5. (a) Large, spherical and porous morphologies of PCL–mannitol nano-aggregates produced in Run A4, (b) PCL nanoparticles are physically dispersed in porous mannitol matrix.

and B1–B4 remain below 20 independent of the mannitol concentration as shown in Fig. 6b. The low CI values denote good particle flowability consistent with the discrete particle morphology observed in Fig. 5a. Importantly, the nano-aggregates can be effectively aerosolized off the entrainment tube as manifested in the high ED values of ≈94%. The FPF values, however, are rather low at 10–14% as a majority of the aerosolized nano-aggregates (40%) deposit in the pre-separator as shown in Fig. 7. The low FPF values indicate that the nano-aggregates tend to agglomerate upon aerosolization.

Particle size distributions of the nano-aggregates produced at 5.0 and 2.5% (w/w) feed concentrations are presented in Fig. 6c and d, respectively. At 5.0% (w/w) feed concentration, the d_G values are in the range of 10–120 μm, whereas at 2.5% (w/w) feed concentration, the d_G values vary within a smaller range of 10–60 μm. Therefore, the particle size distribution is less uniform at higher feed concentrations rendering formulations at low feed concentrations (i.e. Runs B2–B4) more attractive as particle size distributions significantly impact aerosolization, which in turn influence the emitted dose and dosing uniformity. In this regard, Run B2 represents the most ideal formulation as it produces a highly monodisperse distribution with mean d_G of 20 μm. The production yield of Run B2, however, is rather low at 16% making it a less than ideal formulation. A similarly low production yield is also observed in Run B3.

On the other hand, Run B4 produces a relatively similar mean d_G value as that of Run B2, though with a less uniform distribution, but with a significantly higher production yield of 40%. In summary, with the exception of Run A4 in which excessive d_A (≈5.5 μm) is observed, the use of mannitol as the adjuvant results in nano-aggregates having (i) large d_G and low ρ_{tap} values resulting in $d_A \approx 3$–5 μm, (ii) good flowability as demonstrated by CI ≤ 20 and effective aerosolization off the entrainment tube, and (iii) reasonably high production yields (≈40%) and uniform particle size distributions can be achieved at 2.5% (w/w) feed concentration and at N/M ratio of 3:7.

3.3.2. Aqueous re-dispersibility

The ratio of S_f/S_i and the % re-dispersed of the PCL–mannitol nano-aggregates are presented in Fig. 8a and b, respectively. The ratio of S_f/S_i and % re-dispersed and their variations as a function of the mannitol concentration in the feed are found to be independent of the feed concentration. The ratio of S_f/S_i values are reduced from about 4.5 to approximately 1.5 when mannitol concentration in the feed is increased from 0 to 70% (w/w), which signifies increased re-dispersibility attributed to the reduced inter-nanoparticle contacts at higher mannitol concentrations. The decrease in the ratio of S_f/S_i with increasing mannitol concentration in Fig. 8a corresponds to an increased fraction of the nano-aggregates being re-dispersed into primary nanoparticles.

The improved re-dispersions at higher mannitol concentrations are confirmed by the increasing % re-dispersed values with increasing mannitol concentration observed in Fig. 8b. Specifically, the % re-dispersed is increased from 30% in the absence of mannitol in Runs A1 and B1 to ≈85% at 70% (w/w) mannitol concentration in Runs A4 and B4. Importantly, the % re-dispersed of the nano-aggregates produced by SFD represents a significant improvement compared to the PCL–mannitol nano-aggregates produced by spray drying in Kho et al. (2010), which are not at all re-dispersible even at N/M ratio of 1:6. The improved re-dispersion signifies the SFD ability to prevent the occurrence of irreversible nanoparticle coalescences.

Particle size distributions of re-dispersed nanoparticles from Runs B2 and B4 are presented in Fig. 8c. Particle size distribution of re-dispersed nanoparticles from Runs A1–A4 exhibit nearly identical profiles hence they are not presented here for brevity. In Run B2 at 20% (w/w) mannitol concentration, micro-scale fragments (>1500 nm) of the nano-aggregates are present in a significant amount denoting incomplete re-dispersions. As the mannitol concentration is increased to 70% (w/w) in Run B4, the amount of particles recovered in the micro-scale range, though still present, is considerably reduced. A larger fraction of the nano-aggregates are recovered as primary nanoparticles having the same size as the original nanoparticles (≈300 nm). The results indicate that a high mannitol concentration (i.e. 70%, w/w) is needed to achieve complete aggregate re-dispersions.

3.4. PVA as adjuvants

The effects of the nanoparticle to PVA concentration ratio (i.e. N/P ratio) are investigated at two total solid concentrations (i.e. 2.5 and 1.5%, w/w) in the feed. The results of experimental runs at 2.5% (w/w) (i.e. Runs C1–C4) and 1.5% (w/w) (i.e. Runs D1–D4) are presented in Table 2. The N/P ratios are varied by varying the PVA concentration in the feed between 20% and 70% (w/w). Using PVA as adjuvant, SFD at solid concentrations higher than 2.5% (w/w) produces large non-porous particles resulting in $d_A \gg 5$ μm.

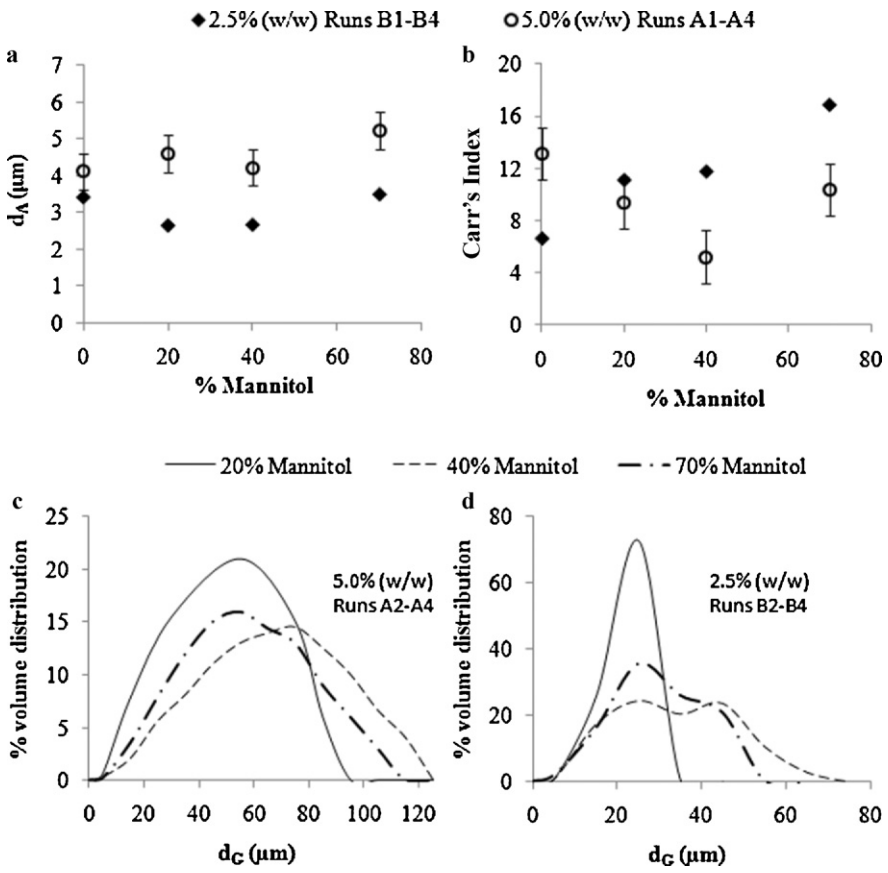

Fig. 6. (a) d_A, (b) CI as a function of mannitol concentration, (c) d_G distributions at 2.5% (w/w) feed concentration, and (d) d_G distributions at 5.0% (w/w) feed concentration.

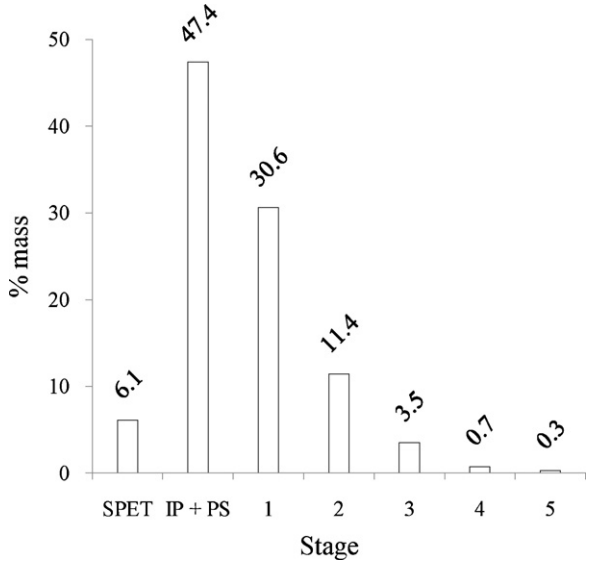

Fig. 7. Particle deposition profile of PCL–mannitol nano-aggregates in NGI (SPET = standardized powder entrainment tube; IP = induction port; PS = pre-separator).

3.4.1. Morphology, density, aerodynamic diameter, flowability, and production yield

In the absence of PVA, nano-aggregates produced at the two feed concentrations are relatively similar in terms of their ρ_{tap} and d_G values, which fall in the range of ≈0.06 g/cm^3 and 16–22 μm, respectively. The production yields of the PVA-free formulations are high at ≈70%, however, they are reduced to ≈30–50% with PVA inclusion. One exception is Run D2 in which the yield is increased to 82%. The production yields are at least 10% higher at 1.5% (w/w) feed concentration than at 2.5% (w/w) in the presence of PVA. In contrast to the results of the PCL–mannitol formulation, the effects of PVA inclusion on the ρ_{tap} and d_G values do not exhibit general trends that are independent of the feed concentration.

At 2.5% (w/w) feed concentration, the ρ_{tap} values are increased from 0.04 to ≈0.06 g/cm^3 with PVA inclusion, whereas the variations in the d_G values are relatively insignificant. On the other hand, at 1.5% (w/w) feed concentration, the PVA inclusion does not have any significant impacts on both the ρ_{tap} and d_G values. On the whole, the d_G values in Runs C2–C4 and D2–D4 are basically unchanged at ≈20 μm. Overall, variations in the ρ_{tap} and d_G values as a function of the N/P ratio are relatively insignificant at these low feed concentrations.

SEM image of the PCL–PVA nano-aggregates in Fig. 9a indicates that PCL–PVA particles are less porous than their PCL–mannitol counterparts shown in Fig. 5a. A close-up view of the particle surface in Fig. 9b indicates that PCL nanoparticles are distributed more closely when PVA is used as the adjuvant, instead of mannitol. Importantly, the porous adjuvant matrix observed in the PCL–mannitol nano-aggregates (Fig. 5b) is not observed in Fig. 9b, which explains for the lower apparent porosity of the PCL–PVA nano-aggregates. The lower porosity is manifested in the overall higher ρ_{tap} values for the PCL–PVA nano-aggregates (i.e. ≈0.04–0.07 g/cm^3 for PCL–PVA versus ≈0.01–0.03 g/cm^3 for PCL–mannitol). Significantly, at feed concentration of 1.5% (w/w), the ρ_{tap} values of the PCL–PVA nano-aggregates (≈0.06 g/cm^3) are still three-fold higher than those of the PCL–mannitol nano-aggregates produced at higher feed concentrations.

In this regard, PCL nanoparticles visible on the aggregate surface in Fig. 9b closely resemble the nanoparticles in the adjuvant-free

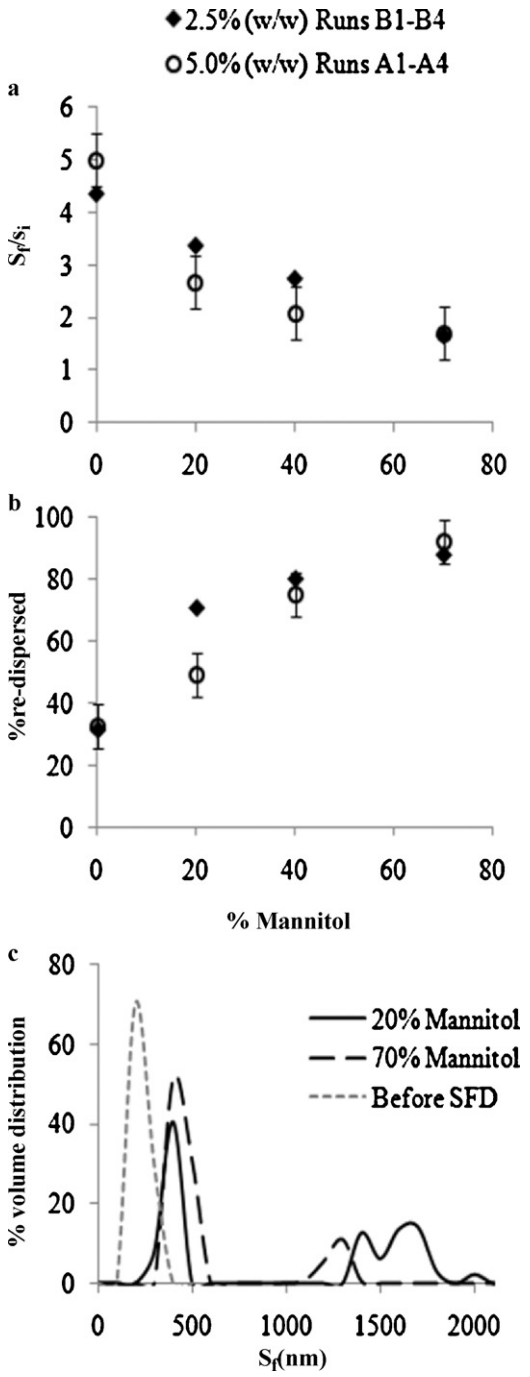

Fig. 8. Aqueous re-dispersibility of PCL–mannitol nano-aggregates (a) ratio of S_f/S_i, (b) % re-dispersed, and (c) size distributions of re-dispersed nano-aggregates.

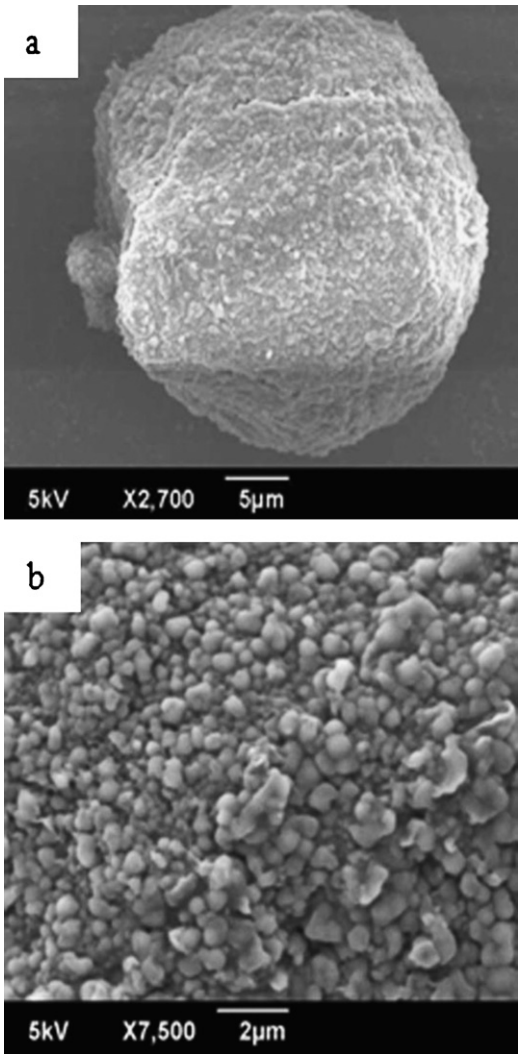

Fig. 9. (a) Large and spherical morphologies of PCL–PVA nano-aggregates produced in Run C3 and (b) closely packed PCL nanoparticles exhibiting larger size due to PVA coatings.

formulation shown in Fig. 3b, except for the larger size (≈500 nm) compared to their original size prior to SFD (≈300 nm). The presence of PVA in the spray-freeze-dried particles has been verified using EDX by examining the carbon to oxygen ratio. As PVA matrix formation is not evident, instead of forming porous matrix like mannitol, PVA is postulated to coat the nanoparticle surface upon lyophilization owed to its surfactant characteristics. The PVA coating provides an explanation for the apparent almost two-fold increase in the nanoparticle size after SFD. In this regard, formation of PVA coating on PCL nanoparticle surface upon lyophilization has previously been reported by Abdelwahed et al. (2006a).

Table 2
Summary of PCL–PVA nano-aggregate experiments.

Run	Feed conc. (w/w)	% PVA (w/w)	N/P ratio	ρ_{tap} (g/cm^3)	d_G (μm)	Yield (%)
C1	2.5%	0	–	0.044	16	70
C2		20	4:1	0.066	18	29
C3		40	3:2	0.062	20	27
C4		70	3:7	0.067	14	36
D1	1.5%	0	–	0.048	22	72
D2		20	4:1	0.050	23	82
D3		40	3:2	0.039	18	50
D4		70	3:7	0.044	21	45

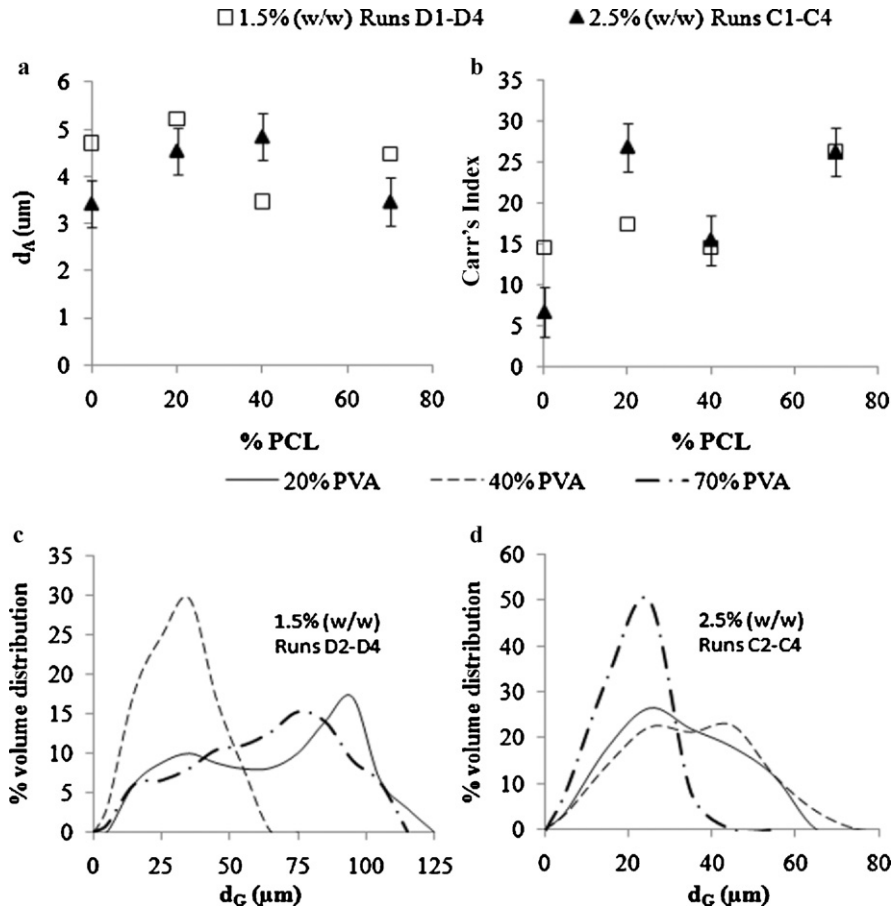

Fig. 10. (a) d_A, (b) CI as a function of PVA concentration, (c) d_G distributions at 1.5% (w/w) feed concentration, and (d) d_G distributions at 2.5% (w/w) feed concentration.

As a result of the difference in their nanoparticle–adjuvant structures, PCL–PVA nano-aggregates exhibit slightly larger d_A values than their PCL–mannitol counterparts despite their relatively similar d_G values. The d_A values of Runs C2–C4 and Runs D2–D4 shown in Fig. 10a are found to vary in the range of 3.5–5.5 μm depending on the feed concentration and the N/P ratio. Certain formulations (e.g. Runs C3 and D2) produce d_A values that are too large for effective lung depositions. In terms of the flowability, PCL–PVA nano-aggregates possess CI values in the range of 15–25 as shown in Fig. 10b, which signifies good flowability similar to the PCL–mannitol nano-aggregates. Not unexpectedly, the PCL–PVA nano-aggregates exhibit similar aerosolization characteristics as their PCL–mannitol counterparts.

With regard to the particle size distribution, nano-aggregates produced at 1.5% and 2.5% (w/w) feed concentrations exhibit wide variations depending on the N/P ratio as shown in Fig. 10c and d, respectively. Nevertheless, highly monodisperse distributions can be obtained at (i) 70% PVA at 2.5% (w/w) feed concentration in Run C4 and (ii) 40% PVA at 1.5% (w/w) feed concentration in Run D3. Importantly, the monodisperse distributions are accompanied by reasonably high production yields (≈40–50%). In summary, similar to the PCL–mannitol formulation, a majority of the PCL–PVA formulations can produce large spherical nano-aggregates having appropriate d_A, good flowability, and reasonable production yields.

3.4.2. Aqueous re-dispersibility

The ratio of S_f/S_i and the % re-dispersed of the PCL–PVA nano-aggregates are presented in Fig. 11a and b, respectively. Similar to the results of the PCL–mannitol formulation, the variations in the ratio of S_f/S_i and % re-dispersed are independent of the feed concentration. The PVA inclusion reduces the ratio of S_f/S_i from ≈5–6 in its absence to ≈1–3 depending on the N/P ratio. The ratio of S_f/S_i decreases and % re-dispersed increases with increasing PVA concentration (i.e. lower N/P ratio), which are again similar to the trends observed in the PCL–mannitol formulations. At 70% PVA concentration in Runs C4 and D4, close to 90% of the nano-aggregates are re-dispersed resulting in the ratio of $S_f/S_i \approx 1$.

Particle size distributions of the re-dispersed nanoparticles from Runs D2 to D3 are presented in Fig. 11c. Particle size distributions of Runs C2–C4 are nearly identical to those of Runs D2–D4 hence they are not presented here for brevity. In Run D2 at 20% PVA concentration, a small amount of micro-scale fragments of the nano-aggregates (>1000 nm) are recovered upon re-dispersion. As the PVA concentration in the feed is increased to 40%, the micro-scale fragments are no longer observed and the size of the re-dispersed nanoparticles all falls within the ≈300–500 nm range. Removal of the micro-scale fragments at 40% adjuvant concentration is not observed in the PCL–mannitol formulation, where fragments in the size range of ≈1000–1500 nm are still present even when 70% of mannitol is used (Fig. 8c).

In this regard, the high crystallization propensity of mannitol may contribute to the poorer aqueous re-dispersibility of the PCL–mannitol formulation. Mechanical stresses exerted by the growing mannitol crystals upon freezing can promote irreversible nanoparticle fusions (Abdelwahed et al., 2006b). Furthermore, crystallized mannitol may undergo phase separations in the cryo-concentrated portion of the frozen nanoparticle suspension (Abdelwahed et al., 2006b), which consequently eliminates the colloidal stabilizing functions of the adjuvant. At low N/M ratios, fewer PCL nanoparticles are dispersed in the vast mannitol matrix,

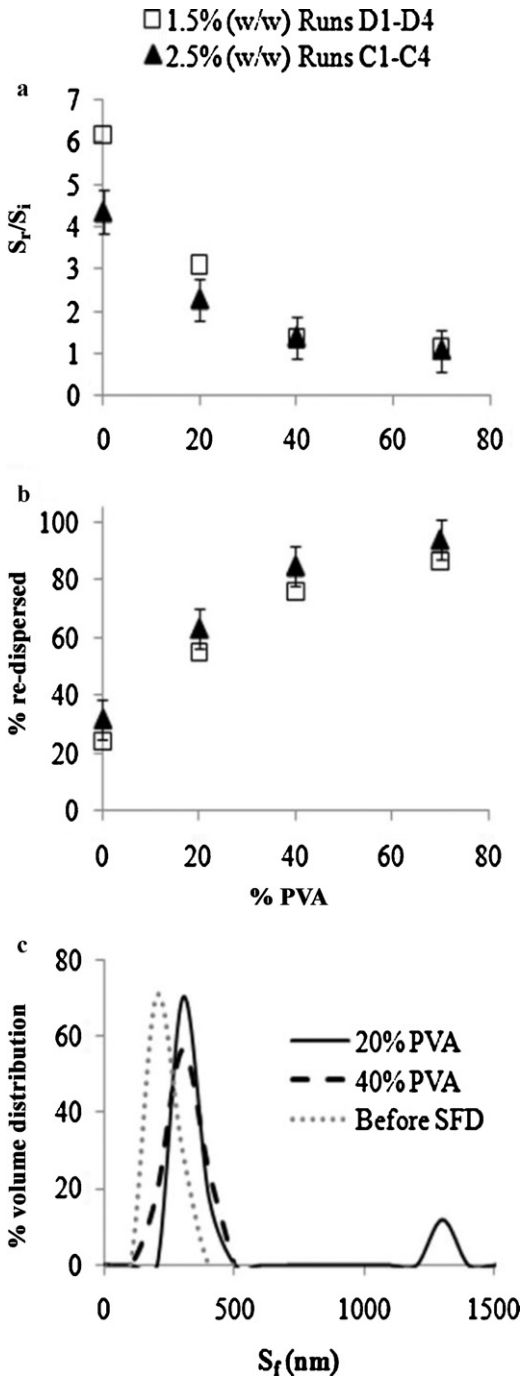

Fig. 11. Aqueous re-dispersibility of PCL–PVA nano-aggregates: (a) ratio of S_f/S_i, (b) % re-dispersed, and (c) size distributions of re-dispersed nano-aggregates.

hence keeping inter-nanoparticle contacts at a minimum resulting in reasonably effective re-dispersions of the nano-aggregates.

In contrast, PVA exists in its glassy state during lyophilization and it has been found to be capable of inhibiting ice nucleation, thereby preventing the formation of ice crystals that exert mechanical stresses on the nanoparticles (Abdelwahed et al., 2006a). Moreover, the presence of PVA coating on the PCL nanoparticle surface can act as stabilizers that minimize inter-nanoparticle contacts during lyophilization. As a result, PCL–PVA nano-aggregates can fully re-disperse into primary nanoparticles more readily (i.e. at lower adjuvant concentration) than the PCL–mannitol nano-aggregates.

As a majority of the formulations can satisfy the d_G and d_A requirements, as well as good flowability, using either mannitol or PVA as adjuvants, the determining nano-aggregate characteristics in selecting the optimal formulation are (i) production yield, (ii) particle size distribution, and (iii) aqueous re-dispersibility. In this regard, the PCL–mannitol formulation in general results in lower production yields (i.e. 15–40%) compared to the PCL–PVA formulation (i.e. 30–80%). Both mannitol and PVA formulations are capable of producing monodisperse particle size distributions (i.e. Runs B2, C4, and D3). However, unlike the PCL–PVA formulation, uniform particle size distributions for the PCL–mannitol formulation are not always accompanied by reasonable production yields and vice versa. Taking all the three characteristics into consideration, the PCL–PVA formulation on the whole is considered to be superior to the PCL–mannitol formulation.

In this regard, Run D3 of the PCL–PVA formulation represents an optimal formulation, where spherical nano-aggregates having mean $d_G \approx 18\,\mu m$, $d_A \approx 4\,\mu m$, CI ≈ 15, production yield ≈ 50%, and monomodal size distribution (d_G mode ≈ 30 μm) are produced. Furthermore, the nano-aggregates produced can be effectively re-dispersed into primary nanoparticles having a monomodal size distribution at ratio of $S_f/S_i \approx 1.3$ and % re-dispersed ≈ 80%. Importantly, compared to the optimal formulation for PCL nano-aggregate productions by spray drying using lactose and leucine as adjuvants presented in Kho et al. (2010), the PCL–PVA formulation in Run D3 is superior in terms of its (i) higher production yield (≈50% vs. 25%), (ii) higher % re-dispersed (≈80% vs. 50%) and lower S_f/S_i ratio (≈1.3 vs. 1.5), and lastly (iii) lower amount of adjuvant needed to achieve effective re-dispersions (≈40% vs. 88% of feed concentration). Therefore, SFD represents a better technique than spray drying to produce inhalable dry-powder aggregates of thermally sensitive polymeric nanoparticles.

4. Conclusion

Dry-powder aggregates of drug-loaded PCL nanoparticles having a large geometric size while remaining in the inhalable size range have been successfully produced using SFD. Mannitol and PVA have been identified in the screening experiments as the two most suitable SFD adjuvants, over lactose and leucine, to serve as cryoprotective agents and to facilitate aqueous re-dispersion of the nanoparticle aggregates. The effects of feed concentration and its adjuvant content on the particle morphology, aerodynamic diameter, aqueous re-dispersibility, flowability, and production yield have been examined. The results indicate that the adjuvant selection dictates the resulting nanoparticle–adjuvant structures, which in turn influence the aerodynamic diameter and aqueous re-dispersibility of the dry-powder aggregates.

Using mannitol as adjuvant, PCL nanoparticles are physically dispersed in porous mannitol matrix, whereas using PVA as adjuvant leads to PVA coating the nanoparticle surface. Both adjuvants nevertheless enhance the aqueous re-dispersibility and produce particles in the inhalable size range having the desired morphology, good flowability, and effective aerosolization off the inhaler. Nevertheless, the fine particle fraction of the aerosolized nano-aggregates still leaves much room for improvement. Experiments on incorporating hydrophobic adjuvants, such as leucine, which can inhibit particle agglomeration upon aerosolization, into the SFD formulation of mannitol and PVA, are currently on-going to improve the fine particle fraction. On the whole, PCL–PVA formulation results in better aqueous re-dispersibility and higher production yield compared to the PCL–mannitol formulation. Taking all the particle characteristics into consideration, PCL–PVA nano-aggregates produced at 1.5% (w/w) feed concentration and 40% (w/w) PVA content have been identified as the optimal formulation.

Acknowledgements

A financial support from Nanyang Technological University's Start-Up Grant (Grant No. SUG 8/07) is gratefully acknowledged.

References

Abdelwahed, W., Degobert, G., Fessi, H., 2006a. A pilot study of freeze drying of poly(epsilon-caprolactone) nanocapsules stabilized by poly(vinyl alcohol): formulation and process optimization. Int. J. Pharm. 309, 178–188.

Abdelwahed, W., Degobert, G., Stainmesse, S., Fessi, H., 2006b. Freeze-drying of nanoparticles: formulation, process and storage considerations. Adv. Drug Deliv. Rev. 58, 1688–1713.

Bi, R., Shao, W., Wang, Q., Zhang, N., 2008. Spray-freeze-dried dry powder inhalation of insulin-loaded liposomes for enhanced pulmonary delivery. J. Drug Target. 16, 639–648.

Cheow, W.S., Hadinoto, K., 2010. Enhancing encapsulation efficiency of highly water-soluble antibiotic in poly(lactic-co-glycolic acid) nanoparticles: modifications of standard nanoparticle preparation methods. Colloids Surf. Physicochem. Eng. Aspects 370, 79–86.

Chono, S., Tanino, T., Seki, T., Morimoto, K., 2006. Influence of particle size on drug delivery to rat alveolar macrophages following pulmonary administration of ciprofloxacin incorporated into liposomes. J. Drug Target. 14, 557–566.

Costantino, H.R., Firouzabadian, L., Hogeland, K., Wu, C., Beganski, C., Carrasquillo, K.G., Córdova, M., Griebenow, K., Zale, S.E., Tracy, M.A., 2000. Protein spray-freeze drying. Effect of atomization conditions on particle size and stability. Pharm. Res. 17, 1374–1383.

Finley, J.H., 1961. Spectrophotometer determination of polyvinyl alcohol in paper coatings. Anal. Chem. 33, 1925.

Grenha, A., Seijo, B., Remuñán-López, C., 2005. Microencapsulated chitosan nanoparticles for lung protein delivery. Eur. J. Pharm. Sci. 25, 427–437.

Hadinoto, K., Cheow, W.S., 2009. Hollow spherical nanoparticulate aggregates as potential ultrasound contrast agent: shell thickness characterization. Drug Dev. Ind. Pharm. 35, 1167–1179.

Her, J.-Y., Song, C.-S., Lee, S.J., Lee, K.-G., 2010. Preparation of kanamycin powder by an optimized spray freeze-drying method. Powder Technol. 199, 159–164.

Hu, J.H., Rogers, T.L., Brown, J., Young, T., Johnston, K.P., Williams, R.O., 2002. Improvement of dissolution rates of poorly water soluble APIs using novel spray freezing into liquid technology. Pharm. Res. 19, 1278–1284.

Kho, K., Cheow, W.S., Lie, R.H., Hadinoto, K., 2010. Aqueous re-dispersibility of spray-dried antibiotic-loaded polycaprolactone nanoparticle aggregates for inhaled anti-biofilm therapy. Powder Technol. 203, 432–439.

Lai, S.K., Wang, Y.Y., Hanes, J., 2009. Mucus-penetrating nanoparticles for drug and gene delivery to mucosal tissues. Adv. Drug Deliv. Rev. 61, 158–171.

Louey, M.D., Van Oort, M., Hickey, A.J., 2006. Standardized entrainment tubes for the evaluation of pharmaceutical dry powder dispersion. J. Aerosol Sci. 37, 1520–1531.

Maa, Y.F., Nguyen, P.A., Sweeney, T., Shire, S.J., Hsu, C., 1999. Protein inhalation powders: spray drying vs spray freeze drying. Pharm. Res. 16, 249–254.

Minne, A., Boireau, H., Horta, M.J., Vanbever, R., 2008. Optimization of the aerosolization properties of an inhalation dry powder based on selection of excipients. Eur. J. Pharm. Biopharm. 70, 839–844.

Misra, R., Acharya, S., Dilnawaz, F., Sahoo, S.K., 2009. Sustained antibacterial activity of doxycycline-loaded poly(D,L-lactide-co-glycolide) and poly(ε-caprolactone) nanoparticles. Nanomedicine 4, 519–530.

Niwa, T., Shimabara, H., Kondo, M., Danjo, K., 2009. Design of porous microparticles with single-micron size by novel spray freeze-drying technique using four-fluid nozzle. Int. J. Pharm. 382, 88–97.

Podczeck, F., 1998. Particle–Particle Adhesion in Pharmaceutical Powder Handling. Imperial College Press, London.

Rogueda, P.G.A., Traini, D., 2007. The nanoscale in pulmonary delivery. Part 1: deposition, fate, toxicology and effects. Expert Opin. Drug Deliv. 4, 595–606.

Rowe, R., Sheskey, P., Quinn, M., 2009. Handbook of Pharmaceutical Excipients, 6th ed. Pharmaceutical Press RPS, London.

Sanchez, J., 1998. Colorimetric assay of alditols in complex biological samples. J. Agric. Food Chem. 46, 157–160.

Sham, J.O.H., Zhang, Y., Finlay, W.H., Roa, W.H., Löbenberg, R., 2004. Formulation and characterization of spray-dried powders containing nanoparticles for aerosol delivery to the lung. Int. J. Pharm. 269, 457–467.

Sheikh, F.A., Barakat, N.A.M., Kanjwal, M.A., Aryal, S., Khil, M.S., Kim, H.Y., 2009. Novel self-assembled amphiphilic poly(epsilon-caprolactone)-grafted-poly(vinyl alcohol) nanoparticles: hydrophobic and hydrophilic drugs carrier nanoparticles. J. Mater. Sci.: Mater. Med. 20, 821–831.

Sinha, V.R., Bansal, K., Kaushik, R., Kumria, R., Trehan, A., 2004. Poly-[epsilon]-caprolactone microspheres and nanospheres: an overview. Int. J. Pharm. 278, 1–23.

Sung, J., Padilla, D., Garcia-Contreras, L., VerBerkmoes, J., Durbin, D., Peloquin, C., Elbert, K., Hickey, A., Edwards, D., 2009. Formulation and pharmacokinetics of self-assembled rifampicin nanoparticle systems for pulmonary delivery. Pharm. Res. 26, 1847–1855.

Sweeney, L.G., Wang, Z., Loebenberg, R., Wong, J.P., Lange, C.F., Finlay, W.H., 2005. Spray-freeze-dried liposomal ciprofloxacin powder for inhaled aerosol drug delivery. Int. J. Pharm. 305, 180–185.